Observation of *B* Decays to Two Kaons

S.-W. Lin,[25] P. Chang,[25] K. Abe,[8] K. Abe,[42] I. Adachi,[8] H. Aihara,[44] D. Anipko,[1] K. Arinstein,[1] V. Aulchenko,[1]
T. Aushev,[17,12] T. Aziz,[40] A. M. Bakich,[39] E. Barberio,[20] A. Bay,[17] I. Bedny,[1] K. Belous,[11] U. Bitenc,[13] I. Bizjak,[13]
S. Blyth,[23] A. Bondar,[1] A. Bozek,[26] M. Bračko,[8,19,13] Y. Chao,[25] A. Chen,[23] K.-F. Chen,[25] W. T. Chen,[23] B. G. Cheon,[3]
R. Chistov,[12] S.-K. Choi,[50] Y. Choi,[38] Y. K. Choi,[38] J. Dalseno,[20] M. Dash,[48] J. Dragic,[8] S. Eidelman,[1] S. Fratina,[13]
N. Gabyshev,[1] T. Gershon,[8] A. Go,[23] G. Gokhroo,[40] B. Golob,[18,13] H. Ha,[15] J. Haba,[8] T. Hara,[31] K. Hayasaka,[21]
H. Hayashii,[22] M. Hazumi,[8] D. Heffernan,[31] Y. Hoshi,[42] S. Hou,[23] W.-S. Hou,[25] Y. B. Hsiung,[25] T. Iijima,[21] K. Ikado,[21]
A. Imoto,[22] K. Inami,[21] A. Ishikawa,[44] H. Ishino,[45] R. Itoh,[8] M. Iwasaki,[44] Y. Iwasaki,[8] H. Kaji,[21] J. H. Kang,[49]
N. Katayama,[8] H. Kawai,[2] T. Kawasaki,[28] H. R. Khan,[45] H. Kichimi,[8] Y. J. Kim,[6] K. Kinoshita,[4] S. Korpar,[19,13]
P. Križan,[18,13] R. Kulasiri,[4] C. C. Kuo,[23] Y.-J. Kwon,[49] J. S. Lange,[5] J. Lee,[36] M. J. Lee,[36] S. E. Lee,[36] T. Lesiak,[26]
A. Limosani,[8] F. Mandl,[10] T. Matsumoto,[46] S. McOnie,[39] W. Mitaroff,[10] K. Miyabayashi,[22] H. Miyake,[31] H. Miyata,[28]
Y. Miyazaki,[21] R. Mizuk,[12] D. Mohapatra,[51] T. Mori,[21] I. Nakamura,[8] E. Nakano,[30] M. Nakao,[8] S. Nishida,[8] O. Nitoh,[47]
S. Noguchi,[22] T. Nozaki,[8] S. Ogawa,[41] T. Ohshima,[21] S. Okuno,[14] S. L. Olsen,[7] Y. Onuki,[34] H. Ozaki,[8] P. Pakhlov,[12]
G. Pakhlova,[12] C. W. Park,[38] H. Park,[16] K. S. Park,[38] R. Pestotnik,[13] L. E. Piilonen,[48] H. Sahoo,[7] Y. Sakai,[8] N. Satoyama,[37]
T. Schietinger,[17] O. Schneider,[17] J. Schümann,[24] A. J. Schwartz,[4] K. Senyo,[21] M. Shapkin,[11] J. B. Singh,[32] A. Sokolov,[11]
A. Somov,[4] N. Soni,[32] S. Stanič,[29] M. Starič,[13] H. Stoeck,[39] T. Sumiyoshi,[46] O. Tajima,[8] F. Takasaki,[8] K. Tamai,[8]
N. Tamura,[28] M. Tanaka,[8] G. N. Taylor,[20] Y. Teramoto,[30] X. C. Tian,[33] I. Tikhomirov,[12] K. Trabelsi,[7] T. Tsukamoto,[8]
S. Uehara,[8] T. Uglov,[12] K. Ueno,[25] Y. Unno,[3] S. Uno,[8] Y. Usov,[1] G. Varner,[7] S. Villa,[17] C. C. Wang,[25] C. H. Wang,[24]
M.-Z. Wang,[25] Y. Watanabe,[45] E. Won,[15] Q. L. Xie,[9] B. D. Yabsley,[39] A. Yamaguchi,[43] Y. Yamashita,[27] M. Yamauchi,[8]
C. C. Zhang,[9] L. M. Zhang,[35] Z. P. Zhang,[35] V. Zhilich,[1] and A. Zupanc[13]

(The Belle Collaboration)

[1]*Budker Institute of Nuclear Physics, Novosibirsk*
[2]*Chiba University, Chiba*
[3]*Hanyang University, Seoul*
[4]*University of Cincinnati, Cincinnati, Ohio 45221*
[5]*Justus-Liebig-Universität Gießen, Gießen*
[6]*The Graduate University for Advanced Studies, Hayama*
[7]*University of Hawaii, Honolulu, Hawaii 96822*
[8]*High Energy Accelerator Research Organization (KEK), Tsukuba*
[9]*Institute of High Energy Physics, Chinese Academy of Sciences, Beijing*
[10]*Institute of High Energy Physics, Vienna*
[11]*Institute of High Energy Physics, Protvino*
[12]*Institute for Theoretical and Experimental Physics, Moscow*
[13]*J. Stefan Institute, Ljubljana*
[14]*Kanagawa University, Yokohama*
[15]*Korea University, Seoul*
[16]*Kyungpook National University, Taegu*
[17]*Swiss Federal Institute of Technology of Lausanne, EPFL, Lausanne*
[18]*University of Ljubljana, Ljubljana*
[19]*University of Maribor, Maribor*
[20]*University of Melbourne, Victoria*
[21]*Nagoya University, Nagoya*
[22]*Nara Women's University, Nara*
[23]*National Central University, Chung-li*
[24]*National United University, Miao Li*
[25]*Department of Physics, National Taiwan University, Taipei*
[26]*H. Niewodniczanski Institute of Nuclear Physics, Krakow*
[27]*Nippon Dental University, Niigata*
[28]*Niigata University, Niigata*
[29]*University of Nova Gorica, Nova Gorica*
[30]*Osaka City University, Osaka*
[31]*Osaka University, Osaka*

^{32}*Panjab University, Chandigarh*
^{33}*Peking University, Beijing*
^{34}*RIKEN BNL Research Center, Upton, New York 11973*
^{35}*University of Science and Technology of China, Hefei*
^{36}*Seoul National University, Seoul*
^{37}*Shinshu University, Nagano*
^{38}*Sungkyunkwan University, Suwon*
^{39}*University of Sydney, Sydney NSW*
^{40}*Tata Institute of Fundamental Research, Bombay*
^{41}*Toho University, Funabashi*
^{42}*Tohoku Gakuin University, Tagajo*
^{43}*Tohoku University, Sendai*
^{44}*Department of Physics, University of Tokyo, Tokyo*
^{45}*Tokyo Institute of Technology, Tokyo*
^{46}*Tokyo Metropolitan University, Tokyo*
^{47}*Tokyo University of Agriculture and Technology, Tokyo*
^{48}*Virginia Polytechnic Institute and State University, Blacksburg, Virginia 24061*
^{49}*Yonsei University, Seoul*
^{50}*Gyeongsang National University, Chinju*
^{51}*Virginia Polytechnic Institute and State University, Blacksburg, Virginia 24061*
(Received 14 December 2006; revised manuscript received 15 March 2007; published 4 May 2007)

Using 449×10^6 $B\bar{B}$ pairs collected with the Belle detector at the KEKB asymmetric-energy e^+e^- collider, we observe clear signals for $B^+ \to \bar{K}^0 K^+$ and $B^0 \to \bar{K}^0 K^0$ decays with 5.3σ and 6.0σ significance, respectively. We measure the branching fractions $\mathcal{B}(B^+ \to \bar{K}^0 K^+) = (1.22^{+0.32+0.13}_{-0.28-0.16}) \times 10^{-6}$ and $\mathcal{B}(B^0 \to \bar{K}^0 K^0) = (0.87^{+0.25}_{-0.20} \pm 0.09) \times 10^{-6}$, and partial-rate asymmetries $A_{CP}(B^+ \to \bar{K}^0 K^+) = 0.13^{+0.23}_{-0.24} \pm 0.02$ and $A_{CP}(B^0 \to \bar{K}^0 K^0) = -0.58^{+0.73}_{-0.66} \pm 0.04$. From a simultaneous fit, we also obtain $\mathcal{B}(B^+ \to K^0 \pi^+) = (22.8^{+0.8}_{-0.7} \pm 1.3) \times 10^{-6}$ and $A_{CP}(B^+ \to K^0 \pi^+) = 0.03 \pm 0.03 \pm 0.01$. The first and second error in the branching fractions and the partial-rate asymmetries are statistical and systematic, respectively. No signal is observed for $B^0 \to K^+ K^-$ decays, and for this branching fraction, we set an upper limit of 4.1×10^{-7} at the 90% confidence level.

All $B \to K\pi$, $\pi\pi$ decays have now been observed [1–4], and direct CP violation has been established in $B^0 \to K^+ \pi^-$ [5,6]. The measurements of these hadronic $b \to s$ and $b \to u$ transitions have provided essential information for our understanding of B decay mechanisms, and are probes for possible new physics. What remains are the $B \to \bar{K}K$ modes, for which measurements with good accuracy are needed. Some measurements for these modes were reported by the Belle and *BABAR* collaborations [7,8].

In this Letter, we report the observation of $B^0 \to \bar{K}^0 K^0$ and $B^+ \to \bar{K}^0 K^+$ decays, which was also recently reported by the *BABAR* collaboration [9]. These decays are expected to be dominated by the loop-induced $b \to d\bar{s}s$ process (called a $b \to d$ penguins) shown in Fig. 1(a). When compared with the $b \to s\bar{d}d$ penguin-dominated $B^0 \to K^0 \pi^+$ decay, these modes are expected to be suppressed by a factor of roughly $1/20$, with branching fractions expected at the 10^{-6} level [10,11]. We also search for $B^0 \to K^+ K^-$, which, at lowest order, arises from a $b \to u$ W-exchange process [Fig. 1(b)] or from final-state interactions [12].

For the decay modes with significant signal, we also measure the partial-rate asymmetry,

$$A_{CP} \equiv \frac{N(\bar{B} \to \bar{f}) - N(B \to f)}{N(\bar{B} \to \bar{f}) + N(B \to f)}, \quad (1)$$

where f denotes $\bar{K}^0 K^0$, $\bar{K}^0 K^+$ or $K^0 \pi^+$. Direct CP violation is expected to be sizable in $B^0 \to \bar{K}^0 K^0$ and $B^+ \to \bar{K}^0 K^+$ decays [10], while mixing-dependent CP violation can be measured in $B^0 \to \bar{K}^0 K^0$ (and $K^+ K^-$) [11].

This analysis is based on a sample of $(449.3 \pm 5.7) \times 10^6 B\bar{B}$ pairs collected with the Belle detector at the KEKB e^+e^- asymmetric-energy (3.5 on 8 GeV) collider [13]. The production rates of $B^+ B^-$ and $B^0 \bar{B}^0$ pairs are assumed to be equal. Throughout this Letter, the inclusion of the charge-conjugate decay is implied, unless explicitly stated otherwise.
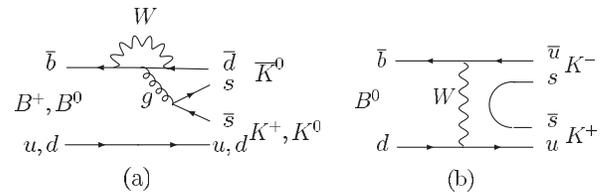

FIG. 1. The $b \to d$ penguin diagram (a) for $B^+ \to \bar{K}^0 K^+$ and $B^0 \to \bar{K}^0 K^0$ modes, and $b \to u$ W-exchange diagram (b) for $B^0 \to K^+ K^-$ decay.

TABLE I. Total number of fitted events (N_t), fitted signal yields, product of efficiencies and subdecay branching fractions ($\mathcal{B}_s$), branching fractions, significance (Σ), and partial-rate asymmetries for individual modes. The first and second error in the branching fractions and the partial-rate asymmetries are statistical and systematic, respectively.

Mode	N_t	Yield	Eff. $\times \mathcal{B}_s$(%)	$\mathcal{B}(10^{-6})$	$\Sigma(\sigma)$	A_{CP}
K^+K^-	391	$2.5^{+5.0}_{-3.7}$	6.18	$0.09^{+0.18}_{-0.13} \pm 0.01\ (<0.41)$	0.6	$\cdots$
$\bar{K}^0 K^+$	2504	$36.6^{+9.7}_{-8.3}$	6.72	$1.22^{+0.32+0.13}_{-0.28-0.16}$	5.3	$0.13^{+0.23}_{-0.24} \pm 0.02$
$K^0 \pi^+$	17905	1252^{+41}_{-39}	12.21	$22.8^{+0.8}_{-0.7} \pm 1.3$	53.1	$0.03 \pm 0.03 \pm 0.01$
$\bar{K}^0 K^0$	792	$23.0^{+6.5}_{-5.4}$	5.89	$0.87^{+0.25}_{-0.20} \pm 0.09$	6.0	$-0.58^{+0.73}_{-0.66} \pm 0.04$

The Belle detector is a large-solid-angle magnetic spectrometer that consists of a silicon vertex detector (SVD), a 50-layer central drift chamber (CDC), an array of aerogel threshold Cherenkov counters (ACC), a barrel-like arrangement of time-of-flight scintillation counters (TOF), and an electromagnetic calorimeter comprised of CsI(Tl) crystals located inside a superconducting solenoid coil that provides a 1.5 T magnetic field. An iron flux-return located outside the coil is instrumented to detect K^0_L mesons and to identify muons. The detector is described in detail elsewhere [14]. Two different inner detector configurations were used. For the first sample of 152×10^6 $B\bar{B}$ pairs (Set I), a 2.0 cm radius beampipe and a 3-layer silicon vertex detector were used; for the latter 297×10^6 $B\bar{B}$ pairs (Set II), a 1.5 cm radius beampipe, a 4-layer silicon detector, and a small-cell inner drift chamber were used [15].

Primary charged tracks are required to have a distance of closest approach to the interaction point (IP) of less than 4 cm in the beam direction (z) and less than 0.1 cm in the transverse plane. Charged kaons and pions are identified using dE/dx information from the CDC and Cherenkov light yields in the ACC, which are combined to form a K-π likelihood ratio, $\mathcal{R}(K/\pi) = \mathcal{L}_K/(\mathcal{L}_K + \mathcal{L}_\pi)$, where $\mathcal{L}_K$ ($\mathcal{L}_\pi$) is the likelihood that the track is a kaon (pion). Charged tracks with $\mathcal{R}(K/\pi) > 0.6\ (<0.4)$ are regarded as kaons (pions) for $B^+ \to \bar{K}^0 K^+$ ($B^+ \to K^0 \pi^+$) decays. A tighter requirement, $\mathcal{R}(K/\pi) > 0.9$, is used for the $B^0 \to K^+ K^-$ selection due to the large background from $B^0 \to K^+ \pi^-$. Furthermore, in all decay modes we reject charged tracks consistent with an electron hypothesis.

Candidate K^0 mesons are observed as $K^0_S \to \pi^+ \pi^-$ decay with the branching fraction taken from Ref. [16]. We pair oppositely charged tracks assuming the pion hypothesis and require the invariant mass of the pair to be within ± 18 MeV/c^2 of the nominal K^0_S mass. The intersection point of the $\pi^+ \pi^-$ pair must be displaced from the IP.

Two variables are used to identify B candidates: the beam-energy constrained mass, $M_{\text{bc}} \equiv \sqrt{E^{*2}_{\text{beam}}/c^4 - p^{*2}_B/c^2}$, and the energy difference, $\Delta E \equiv E^*_B - E^*_{\text{beam}}$, where E^*_{beam} is the run-dependent beam energy and E^*_B and p^*_B are the reconstructed energy and momentum of the B candidates in the center-of-mass (c.m.) frame, respectively. Events with $M_{\text{bc}} > 5.20$ GeV/c^2 and $|\Delta E| < 0.3$ GeV are selected for the analysis.

The dominant background is from $e^+ e^- \to q\bar{q}(q = u, d, s, c)$ continuum events. We use event topology to distinguish the spherically distributed $B\bar{B}$ events from jet-like continuum background. We combine a set of modified Fox-Wolfram moments [17] into a Fisher discriminant. Signal and background likelihoods are formed, based on a GEANT-based [18] Monte Carlo (MC) simulation, from the product of the probability density function (PDF) for the Fisher discriminant and that for the cosine of the angle between the B flight direction and the positron beam. Suppression of continuum is achieved by applying a requirement on a likelihood ratio $\mathcal{R} = \mathcal{L}_{\text{sig}}/(\mathcal{L}_{\text{sig}} + \mathcal{L}_{q\bar{q}})$, where $\mathcal{L}_{\text{sig}}$ ($\mathcal{L}_{q\bar{q}}$) is the signal ($q\bar{q}$) likelihood. Additional continuum background suppression is achieved through use of a B-flavor-tagging algorithm [19], which provides a discrete variable indicating the flavor of the tagging B meson and a quality parameter r, with continuous values ranging from 0 (for no flavor-tagging information) to 1 (for unambiguous flavor assignment). Events with a high value of r are considered well-tagged and hence are unlikely to have originated from continuum processes. We classify events as well-tagged ($r > 0.5$) and poorly-tagged ($r \leq 0.5$), and for each category of Set I and Set II, we determine a continuum suppression requirement for $\mathcal{R}$ that maximizes the value of $N^{\text{exp}}_{\text{sig}}/\sqrt{N^{\text{exp}}_{\text{sig}} + N^{\text{exp}}_{q\bar{q}}}$. Here, $N^{\text{exp}}_{\text{sig}}$ denotes the expected signal yields based on MC simulation and the branching fractions of the previous measurement [7], and $N^{\text{exp}}_{q\bar{q}}$ denotes the expected $q\bar{q}$ yields as estimated from sideband data ($M_{\text{bc}} < 5.26$ GeV/c^2 and $|\Delta E| < 0.3$ GeV).

Background contributions from other $\Upsilon(4S) \to B\bar{B}$ events are investigated with a large MC sample that includes events from $b \to c$ transitions and charmless B decays. After all the selection requirements, no $B\bar{B}$ background is found for the $B^0 \to \bar{K}^0 K^0$ mode. Because of K-π misidentification, large $B^0 \to K^+ \pi^-$ and $B^+ \to K^0 \pi^+$ feed-across backgrounds appear in the $B^0 \to K^+ K^-$ and

$B^+ \to \bar{K}^0 K^+$ samples, respectively. At low ΔE values, a small background contribution from charmless B decays—mainly from $B^+ \to K^+ \pi^0 \bar{K}^0$ ($\bar{B}^0 \to K^{*-}\pi^+$)—is found for the $B^+ \to \bar{K}^0 K^+$ ($B^+ \to K^0 \pi^+$) decay mode. However, experimentally, the $B^+ \to K^+ \pi^0 \bar{K}^0$ mode only has an upper limit.

The signal yields are extracted by performing extended unbinned two-dimensional maximum likelihood (ML) fits to the (M_{bc}, ΔE) distributions in data samples obtained after applying the above selection requirements (see Table I for total events selected). The likelihood for each mode is defined as

$$\mathcal{L} = \exp\left(-\sum_{l,k,j} N_{l,k,j}\right)\prod_i\left(\sum_{l,k,j} N_{l,k,j}\mathcal{P}^i_{l,k,j}\right), \quad (2)$$

$$\mathcal{P}^i_{l,k,j} = \frac{1}{2}[1 - q^i \cdot A_{CPj}]P_{l,k,j}(M^i_{bc}, \Delta E^i), \quad (3)$$

where i is the event identifier, l indicates Set I or Set II, k distinguishes the two r categories, and j runs over all components included in the fitting function—one for the signal and the others for continuum, feed-across, and charmless B backgrounds. $N_{l,k,j}$ represent the number of events, and $P_{l,k,j}(M^i_{bc}, \Delta E^i)$ are the two-dimensional PDFs, which are the same in the two r categories for all fit components except for the continuum background. The parameter q indicates the B-meson flavor: $q = +1(-1)$ for B^+ and B^0 (B^- and $\bar{B}^0$). Unlike $\bar{K}^0 K^+$, the $\bar{K}^0 K^0$ and $K^+ K^-$ channels are not self-tagged and the B meson flavor must be determined from the other B. To account for the effect of $B\bar{B}$ mixing and imperfect tagging, the term A_{CP} for the signal in Eq. (3) has to be replaced by $A_{CP}(1 - 2\chi_d)(1 - 2w_k)$, where $\chi_d = 0.188 \pm 0.003$ [16] is the time-integrated mixing parameter. The χ_d value of continuum events is set to zero. The wrong-tag fraction w_k, which depends on the value of r, is determined from a high statistics sample of self-tagged $B^0 \to D^{*-}\pi^+$, $D^{*-}\rho^+$ and $D^{(*)-}l^+\nu_l$ events [19].

All the signal PDFs [$P_{l,k,j=\text{signal}}(M_{bc}, \Delta E)$] are parameterized by smoothed two-dimensional histograms obtained from correctly reconstructed signal MC based on the Set I and Set II detector configurations. Signal MC events are generated with the PHOTOS [20] simulation package to take into account final-state radiation. Since the M_{bc} signal distribution is dominated by the beam-energy spread, we apply small corrections to the signal peak position and resolution determined using $B^+ \to \bar{D}^0 \pi^+$ from data ($\bar{D}^0 \to K^0_S \pi^+ \pi^-$ is used for the $\bar{K}^0 K^0$ mode, while $\bar{D}^0 \to K^+ \pi^-$ is used for the other three modes) with small mode-dependent corrections obtained from MC. The resolution for the ΔE distribution is calibrated using the invariant mass distributions of high momentum ($p_{Lab} > 3$ GeV/c) D mesons. The decay mode $\bar{D}^0 \to K^+ \pi^-$ is used for $B^0 \to K^+ K^-$, $D^+ \to K^0_S \pi^+$ for $B^+ \to K^0 \pi^+$ and $\bar{D}^0 \to K^0_S \pi^+ \pi^-$ for $B^0 \to \bar{K}^0 K^0$.

The continuum background PDF is described by a product of a linear function for ΔE and an ARGUS function, $f(x) = x\sqrt{1 - x^2}\exp[-\xi(1 - x^2)]$, where $x = M_{bc}c^2/E^*_{beam}$ [21]. The overall normalization, ΔE slope and ARGUS parameter ξ are free parameters in the fit. The background PDFs for charmless B decays for the $K^0 \pi^+$ and $\bar{K}^0 K^+$ modes are both modeled by smoothed two-dimensional histograms obtained from a large MC sample. We also use smoothed two-dimensional histograms to describe the feed-across backgrounds for the $K^+ K^-$ ($\bar{K}^0 K^+$) mode, since the background $K^+ \pi^-$ ($K^0 \pi^+$) events have (M_{bc}, ΔE) shapes similar to the signal, except for the ΔE peak positions shifted by $\simeq 45$ MeV. We perform a simultaneous fit for $B^+ \to \bar{K}^0 K^+$ and $B^+ \to K^0 \pi^+$, since these two decay modes feed into each other. Because the branching fraction of $B^0 \to K^+ K^-$ is small, we also treat the yields of $K^+ \pi^-$ feed-across events as free parameters in the fit.

When likelihood fits are performed, all the $N_{l,k,j}$ are allowed to float except for the feed-across backgrounds in the $\bar{K}^0 K^+$ and $K^0 \pi^+$ modes. The M_{bc} and ΔE projections of the fits are shown in Fig. 2. The branching fraction in each mode is calculated by dividing the efficiency-
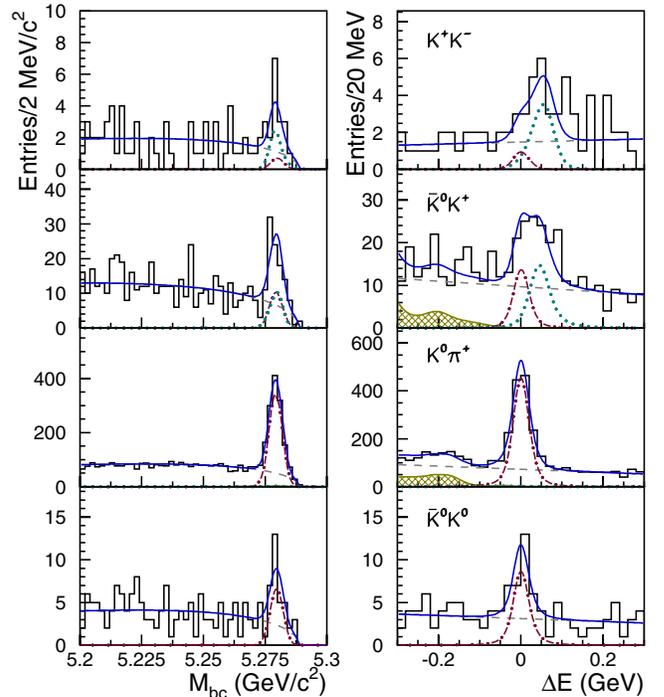

FIG. 2 (color online). M_{bc} (left) and ΔE (right) distributions for $B \to K^+ K^-$, $\bar{K}^0 K^+$, $K^0 \pi^+$, and $\bar{K}^0 K^0$ candidates. The histograms show the data, while the curves represent the various components from the fit: signal (dot-dashed line), continuum (dashed line), charmless B decays (hatched line), feed-across background from misidentification (dotted line), and sum of all components (solid line). The M_{bc} and ΔE projections of the fits are for events that have $|\Delta E| < 0.06$ GeV (left) and 5.271 GeV/$c^2 < M_{bc} < 5.289$ GeV/c^2 (right), respectively.

corrected total signal yield by the number of $B\bar{B}$ pairs. In Table I, a sum of fitted signal yields and the average efficiency are listed.

The fitting systematic errors include the signal PDF modeling, which we estimate from the deviations after varying each parameter of the signal PDFs by 1 standard deviation in the calibration factors, and the modeling of the charmless B background. Since the ΔE values of the charmless B events are typically less than -0.12 GeV, the systematic error due to the modeling of the charmless B background is evaluated by requiring $\Delta E > -0.12$ GeV. At each step, the yield deviation is added in quadrature to provide the fitting systematic errors, and the statistical significance is computed by taking the square root of the difference between the value of $-2\ln\mathcal{L}$ for the best fit and that for zero signal yield. For $B^+ \to \bar{K}^0 K^+$, systematic uncertainty is included in the significance calculation by varying the feed-across background (which is the dominant uncertainty) by 1σ in the direction that lowers the significance. For the other decay modes, the effect of systematic uncertainty on the significance is negligible.

The MC-data efficiency difference due to the requirement on the likelihood ratio $\mathcal{R}$ is investigated using the $B^+ \to \bar{D}^0 \pi^+$ ($\bar{D}^0 \to K_S^0 \pi^+ \pi^-$ for $\bar{K}^0 K^0$ and $\bar{D}^0 \to K^+ \pi^-$ for the others) samples. The systematic error due to the charged-track reconstruction efficiency is estimated to be 1% per track using partially reconstructed D^* events. The systematic error due to $\mathcal{R}(K/\pi)$ selection is 1.3% for pions and 1.5% for kaons, respectively. Due to the tighter $\mathcal{R}(K/\pi)$ selection of kaons in the $K^+ K^-$ mode, the assigned systematic uncertainty is 1.9% per kaon track. The K_S^0 reconstruction is verified by comparing the ratio of $D^+ \to K_S^0 \pi^+$ and $D^+ \to K^- \pi^+ \pi^+$ yields with the MC expectation. We vary the yields of feed-across background by $\pm1\sigma$ to check the effect from the constraint on the feed-across background. Possible systematic uncertainties due to the description of final-state radiation have been studied by comparing the latest theoretical calculations with the PHOTOS MC [22]. These uncertainties were found to be negligible and thus no systematic error is assigned due to PHOTOS. The systematic error due to the uncertainty in the total number of $B\bar{B}$ pairs is 1.3% and the error due to signal MC statistics is in the range 0.8–1.1%. The final systematic errors are obtained by quadratically summing the errors due to the reconstruction efficiency and the fitting systematics. The summary of the systematic errors is shown in Table II.

The detector bias is the dominant systematic error for $A_{CP}(B^+ \to \bar{K}^0 K^+)$ and $A_{CP}(B^+ \to K^0\pi^+)$; the systematic uncertainties evaluated from the partial-rate asymmetry of the continuum background are 0.02 and 0.01 for these two modes, respectively. The systematic errors for $A_{CP}(B^0 \to \bar{K}^0 K^0)$ are estimated by varying the fitting parameters by $\pm1\sigma$. We include also the errors due to w_k, χ_d and tagside interference [23] and obtain a total systematic error of 0.04.

TABLE II. Summary of systematic errors, given in percent.

	K^+K^-	$\bar{K}^0K^+$	$K^0\pi^+$	$\bar{K}^0K^0$
Signal PDF	$^{+1.3}_{-1.4}$	±0.2	±0.2	$^{+0.5}_{-0.6}$
Charmless B background	0.0	-0.9	-0.1	0.0
$\mathcal{R}$ requirement	±0.8	±1.4	±1.1	±3.3
Tracking	±2.0	±1.0	±1.0	0.0
$\mathcal{R}(K/\pi)$ requirement	±3.9	±1.5	±1.3	0.0
K_S^0 reconstruction	0.0	±4.9	±4.9	±9.8
No. of feed-across	0.0	$^{+9.4}_{-11.9}$	$^{+0.2}_{-0.4}$	0.0
No. of $B\bar{B}$	±1.3	±1.3	±1.3	±1.3
Signal MC statistics	±1.1	±1.1	±0.8	±0.8
Sum	$^{+4.9}_{-5.0}$	$^{+11.0}_{-13.2}$	±5.5	±10.5

In summary, using a data sample with 449×10^6 $B\bar{B}$ pairs, we observe $B^+ \to \bar{K}^0 K^+$ and $B^0 \to \bar{K}^0 K^0$ with branching fractions $\mathcal{B}(B^+ \to \bar{K}^0 K^+) = (1.22^{+0.32+0.13}_{-0.28-0.16}) \times 10^{-6}$ and $\mathcal{B}(B^0 \to \bar{K}^0 K^0) = (0.87^{+0.25}_{-0.20} \pm 0.09) \times 10^{-6}$. The corresponding partial-rate asymmetries are $A_{CP}(B^+ \to \bar{K}^0 K^+) = 0.13^{+0.23}_{-0.24} \pm 0.02$ and $A_{CP}(B^0 \to \bar{K}^0 K^0) = -0.58^{+0.73}_{-0.66} \pm 0.04$. In addition, we improve the measurements of the branching fraction and partial-rate asymmetry for the decay $B^+ \to K^0\pi^+$: $\mathcal{B}(B^+ \to K^0\pi^+) = (22.8^{+0.8}_{-0.7} \pm 1.3) \times 10^{-6}$ and $A_{CP}(B^+ \to K^0\pi^+) = 0.03 \pm 0.03 \pm 0.01$. Our measurements are consistent with previous results [1,7,8]. The new results, except for $\mathcal{B}(B^0 \to K^+ K^-)$ and $A_{CP}(B^0 \to \bar{K}^0 K^0)$, have better precision than previously measured values. Our results agree with some theoretical predictions [10,11,24–26]. No signal is observed for $B^0 \to K^+ K^-$, and we set an upper limit of 4.1×10^{-7} at the 90% confidence level using the Feldman-Cousins approach [27].

[1] Y. Chao *et al.* (Belle Collaboration), Phys. Rev. D **69**, 111102 (2004).
[2] B. Aubert *et al.* (*BABAR* Collaboration), Phys. Rev. Lett. **89**, 281802 (2002); **92**, 201802 (2004).
[3] Y. Chao *et al.* (Belle Collaboration), Phys. Rev. Lett. **94**, 181803 (2005).
[4] B. Aubert *et al.* (*BABAR* Collaboration), Phys. Rev. Lett. **94**, 181802 (2005).

[5] Y. Chao *et al.* (Belle Collaboration), Phys. Rev. Lett. **93,** 191802 (2004); K. Abe *et al.* (Belle Collaboration), arXiv:hep-ex/0507045.

[6] B. Aubert *et al.* (*BABAR* Collaboration), Phys. Rev. Lett. **93,** 131801 (2004).

[7] K. Abe *et al.* (Belle Collaboration), Phys. Rev. Lett. **95,** 231802 (2005).

[8] B. Aubert *et al.* (*BABAR* Collaboration), Phys. Rev. Lett. **95,** 221801 (2005).

[9] B. Aubert *et al.* (*BABAR* Collaboration), Phys. Rev. Lett. **97,** 171805 (2006).

[10] J.-M. Gérard and W.-S. Hou, Phys. Lett. B **253,** 478 (1991).

[11] R. Fleischer, Phys. Lett. B **341,** 205 (1994).

[12] A. J. Buras, R. Fleischer, and T. Mannel, Nucl. Phys. B **533,** 3 (1998); C.-K. Chua, W.-S. Hou, and K.-C. Yang, Mod. Phys. Lett. A **18,** 1763 (2003); S. Barshay, L. M. Sehgal, and J. van Leusen, Phys. Lett. B **596,** 240 (2004).

[13] S. Kurokawa and E. Kikutani, Nucl. Instrum. Methods Phys. Res., Sect. A **499,** 1 (2003), and other papers included in this volume.

[14] A. Abashian *et al.* (Belle Collaboration), Nucl. Instrum. Methods Phys. Res., Sect. A **479,** 117 (2002).

[15] Z. Natkaniec *et al.* (Belle SVD2 Group), Nucl. Instrum. Methods Phys. Res., Sect. A **560,** 1 (2006).

[16] W.-M. Yao *et al.* (Particle Data Group), J. Phys. G **33,** 1 (2006).

[17] G. C. Fox and S. Wolfram, Phys. Rev. Lett. **41,** 1581 (1978); The modified moments used in this paper are described in, S. H. Lee *et al.* (Belle Collaboration), Phys. Rev. Lett. **91,** 261801 (2003).

[18] R. Brun *et al.*, GEANT 3.21, CERN Report No. DD/EE/ 84-1, 1987.

[19] H. Kakuno *et al.*, Nucl. Instrum. Methods Phys. Res., Sect. A **533,** 516 (2004).

[20] E. Barberio and Z. Was, Comput. Phys. Commun. **79,** 291 (1994); P. Golonka and Z. Was, arXiv:hep-ph/0506026. We use PHOTOS version 2.13 allowing the emission of up to two photons, with an energy cutoff at 1% of the energy available for photon emission (i.e., approximately 26 MeV for the first emitted photon). PHOTOS also takes into account interference between charged final-state particles.

[21] H. Albrecht *et al.* (ARGUS Collaboration), Phys. Lett. B **241,** 278 (1990).

[22] G. Nanava and Z. Was, arXiv:hep-ph/0607019.

[23] O. Long, M. Baak, R. N. Cahn, and D. Kirkby, Phys. Rev. D **68,** 034010 (2003).

[24] C.-H. Chen and H.-N. Li, Phys. Rev. D **63,** 014003 (2000).

[25] M. Beneke and M. Neubert, Nucl. Phys. B **675,** 333 (2003); C.-W. Chiang, M. Gronau, J. L. Rosner, and D. A. Suprun, Phys. Rev. D **70,** 034020 (2004).

[26] R. Fleischer and S. Recksiegel, Eur. Phys. J. C **38,** 251 (2004); A. K. Giri and R. Mohanta, J. High Energy Phys. 11 (2004) 084.

[27] G. J. Feldman and R. D. Cousins, Phys. Rev. D **57,** 3873 (1998).